JEE Journal of Ecological Engineering

Journal of Ecological Engineering, 2027, 28(1), 113–127
https://doi.org/10.12911/22998993/236128
ISSN 2299–8993, License CC-BY 4.0

Received: 2026.08.23
Accepted: 2026.11.16
Published: 2026.12.01

Pilot-scale hydrodynamic cavitation for microbial reduction in slaughterhouse wastewater

Jorge Alberto Neira Tavera[1*], Yecid Alfonso Muñoz Maldonado[1], Víctor Alfonso Solarte David[1], Freddy Alexander Jara Mora[2], Luis Eduardo Cobos Ramírez[2], Sandra Johana Benítez Muñoz[2], Alix Estela Yusara Contreras Gómez[3], Inés Hernández Celi[3], Frank Carlos Vargas Tangua[2], Wilson Gamboa Contreras[2]

[1] Faculty of Engineering, Universidad Autónoma de Bucaramanga (UNAB), Avenida 42 No. 48–11, El Jardín, Bucaramanga, Santander, Colombia
[2] Department of Research, Fundación Universitaria de San Gil (UNISANGIL), Campus Universitario, Km 2 vía San Gil–Charalá, San Gil, Santander, Colombia
[3] Universidad Santo Tomás, Seccional Bucaramanga, Carrera 18 No. 9–27, Bucaramanga, Santander, Colombia
* Corresponding author's e-mail: jneira479@unab.edu.com

ABSTRACT

Hydrodynamic cavitation (HC) was examined as a post-biological polishing step for cattle-slaughterhouse wastewater at Villanueva, Santander, Colombia. Five field batches (270 L each), collected on different days and at different times of day during a three-month campaign, were recirculated independently for 60 min through a fin-type restriction. Samples collected before treatment and after 30 and 60 min were analyzed in triplicate for two coliform assays, an aerobic-mesophile count, and a combined mold/yeast count. The loop operated at mean inlet pressure and flow of 680.3 ± 2.9 kPa and 5.975 ± 0.178 L s^{-1}, respectively. By 60 min, the mean bulk-temperature increase was 19.5 ± 1.345 °C and the calculated circulation was 79.68 ± 9.22 tank-volume cycles. Pressure and flow showed no significant time effect. Thirty-minute mean reductions ranged from 26.09% (molds and yeasts) to 98.311% (total coliforms). At 60 min, no colony was recovered for either coliform assay or for aerobic mesophiles under the specified culture procedure; molds and yeasts decreased by 95.0 ± 7.071%. Those zero-colony observations denote assay-bounded non-detection and are not evidence of sterility. The five trials show a reproducible direction of microbial change in this high-strength secondary effluent. Since electricity use, cavitation number, and post-treatment regrowth were not measured, energetic or sustainability performance cannot be inferred.

Keywords: cattle-processing effluent, culture counts, fin-type restriction, hydraulic recirculation, tertiary polishing.

INTRODUCTION

Slaughterhouse wastewater is intrinsically variable because blood and soluble proteins, fat, rumen residues, detergents, and wash water enter the drain in proportions that change with animal species, daily throughput, product recovery, sanitation routines, and water consumption (Aziz et al., 2019; Dos Santos Pereira et al., 2024). This variability governs both the feasibility of water reuse and the load received by downstream treatment (Asgharnejad et al., 2021). The broad chemical oxygen demand (COD), biochemical oxygen demand (BOD), and solids intervals reported for poultry-processing facilities show why the sector cannot be treated as a single wastewater type (Yaakob et al., 2018). For cavitation-based polishing, the same variability is part of the exposure because dissolved matter and particles may alter

the flow environment, shield microorganisms, or consume short-lived oxidants.

Microbial risk therefore remains relevant after considering organic and solids loads. Abattoir discharges have been associated with deterioration of receiving-water physicochemistry (Igbinosa and Uwidia, 2018), and culture of meat-industry effluent has recovered fecal organisms, including antimicrobial-resistant isolates (Stošić et al., 2016). A treatment train intended for discharge or reuse must consequently address the surviving microbial fraction as well as carbon, nutrients, and solids. Upstream treatment removes much of the particulate and biodegradable load but does not by itself define the microbial quality of the final effluent. Screening, flotation, anaerobic conversion, and aerobic treatment are commonly followed or complemented by membranes and advanced oxidation; these operations function as treatment trains rather than universal substitutes for one another (Bustillo-Lecompte and Mehrvar, 2017). Even a well-performing anaerobic–anoxic–aerobic arrangement may combine high COD removal with incomplete nitrogen removal (Lopes et al., 2022), and full-scale performance depends on continuity across the plant (Michael et al., 2020). The present experiment therefore begins after secondary clarification and evaluates microbial polishing, not removal of the raw-wastewater organic and solids load.

Available polishing barriers are also matrix-sensitive. Turbidity, suspended particles, organic carbon, and organism type change the exposure required for chlorination, ozone, and ultraviolet (UV) disinfection (Collivignarelli et al., 2018; Costa et al., 2026). For oxidative treatment, disappearance of a target does not resolve whether transformation products remain relevant (von Gunten, 2018). Elsaidy et al. (2022) addressed chlorine demand and by-product formation in carbon-rich slaughterhouse water with a lower-hypochlorite approach, whereas UV avoids a chemical residual but may be limited by particle shielding and post-treatment reactivation (González et al., 2023). These constraints motivate evaluation of hydrodynamic cavitation (HC) in real effluent without assuming an intrinsic safety or cost advantage.

HC creates cavities when local pressure in a moving liquid falls sufficiently; collapse follows as pressure recovers. Candidate stresses on microorganisms include pressure pulses, shear, microjets, localized heating, and reactive chemical conditions (Carpenter et al., 2017). Their balance changes with the operating point, liquid composition, device geometry, and the position of a bubble relative to a boundary. Dular et al. (2016) and Zupanc et al. (2019) consequently interpret HC inactivation through interacting physical and chemical effects. Because the present experiment did not measure those effects separately, apparatus and operating conditions are needed to interpret the biological outcome.

Reactor geometry is a first source of that dependence. Orifices, Venturi sections, and vortex diodes create low-pressure regions as liquid crosses a fixed restriction, whereas rotor–stator units create a moving pressure field. Reviews identify throat dimensions, diffuser angle, pressure recovery, flow, and cavitation regime as design-sensitive variables (Chen et al., 2023; Zheng et al., 2022). Computational fluid dynamics (CFD) studies predict different vapor patterns and stresses after small geometric changes (Gostiša et al., 2022; Hong et al., 2022), but the predicted field still requires experimental verification. Scale is not neutral: at the same specific energy, Gode et al. (2023) found that enlarging a vortex device reduced performance. A device-specific description is therefore required before microbial change is interpreted at pilot scale.

Microbial results confirm this device dependence. A vortex diode produced different responses for *Escherichia coli* and *Staphylococcus aureus*, and its effective pressure drop differed from that of an orifice (Jain et al., 2019). Burzio et al. (2020) incorporated cavitation number into an orifice-reactor analysis, but geometry and scale remained relevant. Šarc et al. (2017) further showed that cavitation number is ambiguous without its pressure reference, dimensions, temperature, and liquid properties. In a rotor–stator system, *E. coli* and *Enterococcus faecalis* declined rapidly in synthetic water, with energy demand dependent on configuration (Cerecedo et al., 2018). These studies explain the expected apparatus dependence but provide no direct benchmark for particulate slaughterhouse secondary effluent treated in a fin reactor.

Exposure must also include passage count and thermal history. In a 15 L simulated-effluent experiment, rotor speed and pump setting changed the temperature trajectory, which Sun et al. (2018) implicated in the *E. coli* result. For a radial-groove device, Hou et al. (2023) showed that flow affected both cavitation state and the frequency of bacterial passage through the active region. Xue et al. (2025) found additional effects of groove shape and dimensions on cavitation

intensity and *E. coli* response. Treatment time is therefore interpretable only with reactor geometry, circulation rate, and temperature history; all three are reported for the present loop.

The analytical target is another source of variation. MS2 is a bacteriophage commonly used as a surrogate for norovirus; small HC reactors produced more than four-log inactivation of this virus, but pathways proposed for relatively simple water cannot be assigned automatically to bacteria carried by particles (Kosel et al., 2017). *Legionella pneumophila*, *E. coli*, and *Bacillus subtilis* responded differently under supercavitation (Šarc et al., 2018). At the single-bubble scale, Pandur et al. (2023) located *E. coli* damage within a narrow near-wall microjet interaction zone rather than uniformly throughout the vessel. Organism, matrix, reactor, exposure, and enumeration method must therefore accompany any reported reduction.

Co-treatments further limit cross-study inference. Hydrogen peroxide improved lake-water treatment compared with HC alone while changing the chemistry and operating envelope (Patil et al., 2023). Peppermint oil intensified treatment of resistant bacteria in vortex and orifice devices, making the intervention a hybrid process (Mane et al., 2020). In peanut milk, HC and high-intensity ultrasound produced different changes in total plate count and molds/yeasts (Salve et al., 2019). These distinctions explain why reviews call for measurements in real effluent, at relevant scale, with energy recorded directly (Agarkoti et al., 2021; Sun et al., 2024).

Slaughterhouse-polishing studies provide the closest application context, although their unit operations differ. Membranes may yield high-quality water when pretreatment and fouling are controlled (Fatima et al., 2021; Goswami and Pugazhenthi, 2020). Broad microbial removal by electrocoagulation followed by ultrafiltration and UV reflects the contribution of an entire train (Meiramkulova et al., 2021). UV-C performance after biological treatment depends on the optical and microbial load passed forward (Svierzoski et al., 2021), whereas electrocoagulation adds current-density, electrode-consumption, and sludge-management requirements (Sandoval et al., 2024; Zarei et al., 2018). In real abattoir effluent, acoustic cavitation gave a stronger response when coupled with ozone (Alfonso-Muniozguren et al., 2020). Valid comparison across these studies requires, at minimum, initial count, analytical endpoint, volume, treatment inputs, and energy basis.

Across HC studies, pressure, recirculation time, reactor arrangement, and direct measurement of reactive species have each changed the interpretation of process performance. Lebiocka (2020) found that municipal-wastewater solubilization across 3.5–7 bar varied with pressure and recirculation time. Ahmed et al. (2025) reported a joint influence of pressure and orifice arrangement on sludge disintegration, with greater energy demand during longer operation. On related pilot equipment, Cobos Ramírez et al. (2026) followed the same four culture endpoints in urban wastewater, while Sikora et al. (2026) independently measured hydroxyl-radical formation. An institutional monograph also presented a descriptive summary of fin-reactor trials with 270 L of slaughterhouse wastewater (Muñoz Neira et al., 2025). These reports show that reactor geometry, matrix, operating conditions, analytical thresholds, and experimental replication must accompany a microbial outcome before it can be interpreted or transferred to another application.

A specific evidence gap nevertheless remains: the literature has not provided a batch-replicated assessment of a fin-type restriction used without an added oxidant to polish real, high-strength secondary slaughterhouse effluent while microbial, hydraulic, and thermal responses are recorded together. Bench studies commonly use simpler water, smaller volumes, or a single target organism, whereas the previous institutional summary did not establish the analytical and inferential detail required to evaluate repeatability across field batches (Muñoz Neira et al., 2025; Yadav et al., 2021). The present study addresses that gap through five independent 270 L batches collected over three months on different days and at different times of day. Each batch was sampled at 0, 30, and 60 min for two coliform assays, aerobic mesophiles, and molds/yeasts while inlet pressure, flow, bulk temperature, and nominal circulation were recorded in parallel. The novelty resides in combining a real-effluent pilot volume, repeated field batches, four culture endpoints, and a concurrent hydraulic–thermal record within one analysis. We expected culture counts to decline as passage accumulated while pressure and flow remained stable. The study tests feasibility and repeatability within this operating envelope; claims of sterility, a single inactivation pathway, energy performance, or superiority over established barriers fall outside the evidence collected.

MATERIALS AND METHODS

Wastewater origin and experimental unit

The experimental influent was collected at the outlet of the secondary clarifier of a cattle-processing plant in Villanueva, Santander, Colombia. The preceding treatment train comprised preliminary screening, recirculated anaerobic hydrolysis, an oxidation ditch, and secondary clarification (Figure 2a). The experimental campaign extended over three months and comprised five separate 60 min HC runs (5 h of active treatment in total). Each run was conducted on a different day and at a different time of day using a newly collected 270 L batch from the secondary-clarifier outlet; batches were not pooled. This schedule introduced temporal variation in the field matrix, but the five runs were not balanced across predefined time blocks and therefore do not support a separate day-of-week or time-of-day effect. Plant records described a typical weekly throughput of about 260 cattle and approximately 39,000 L of wastewater treated per week. These weekly plant descriptors are distinct from the three-month experimental campaign.

The secondary-clarifier outlet was the plant-level collection point and the receiving tank was the pilot-level sampling location (Figure 2a–b). For each batch, the 0 min aliquot was withdrawn from the filled receiving tank before recirculation; the 30 and 60 min aliquots were withdrawn from the same batch after the corresponding elapsed recirculation time. Samples were processed immediately and each assay was measured in triplicate. Because collection followed biological treatment, the response examined here is a polishing response; raw-wastewater solids and organic-load removal were outside the experiment. Each batch constituted one independent experimental unit, and within-batch analytical replication was kept separate when variability was summarized.

Fin reactor and recirculating pilot loop

The cavitation element was a fin-shaped flow restriction developed at UNISANGIL. Figure 1 is relevant because it identifies the intended hydrodynamic sequence within this geometry: upstream pressurization, a restricted low-pressure region around the fin where cavity formation is expected, and downstream pressure recovery. The computed field was used to explain the design and locate the active restriction, not to represent pressure measured during the field runs. Figure 2 places the HC loop after secondary clarification and shows the receiving tank, pump, upstream and downstream pressure gauges, flow meter, return line, control valves, and aliquot sequence. Effluent leaving the fin returned to the tank, so the same batch traversed the element repeatedly during the 60 min run. Figure 1 therefore provides qualitative design context rather than operating evidence. Inlet pressure during the runs came from the upstream gauge. Cavitation number was

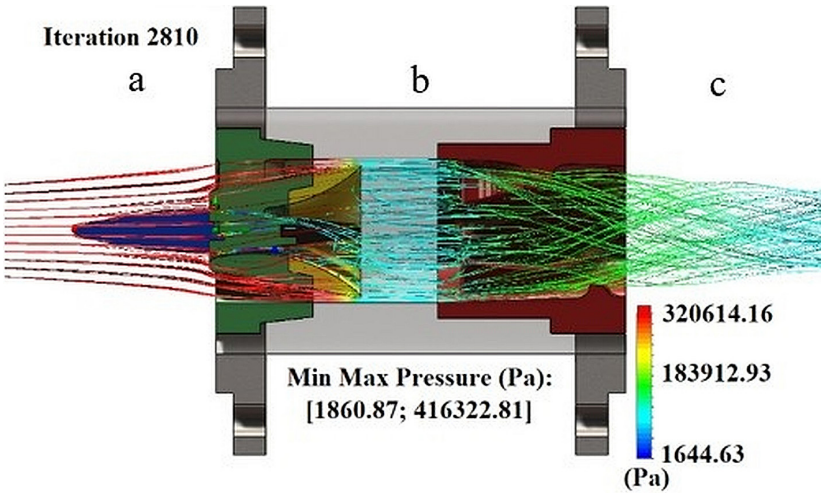

Figure 1. Simulated pressure field used to locate the hydrodynamic sequence in the fin restriction: (a) upstream pressurization, (b) restricted low-pressure zone where cavity formation is expected, and (c) downstream recovery. The displayed contour scale and the model-wide pressure extrema are reproduced separately from the archived simulation output. The simulation provides design context only; field pressure was measured independently with the installed gauges

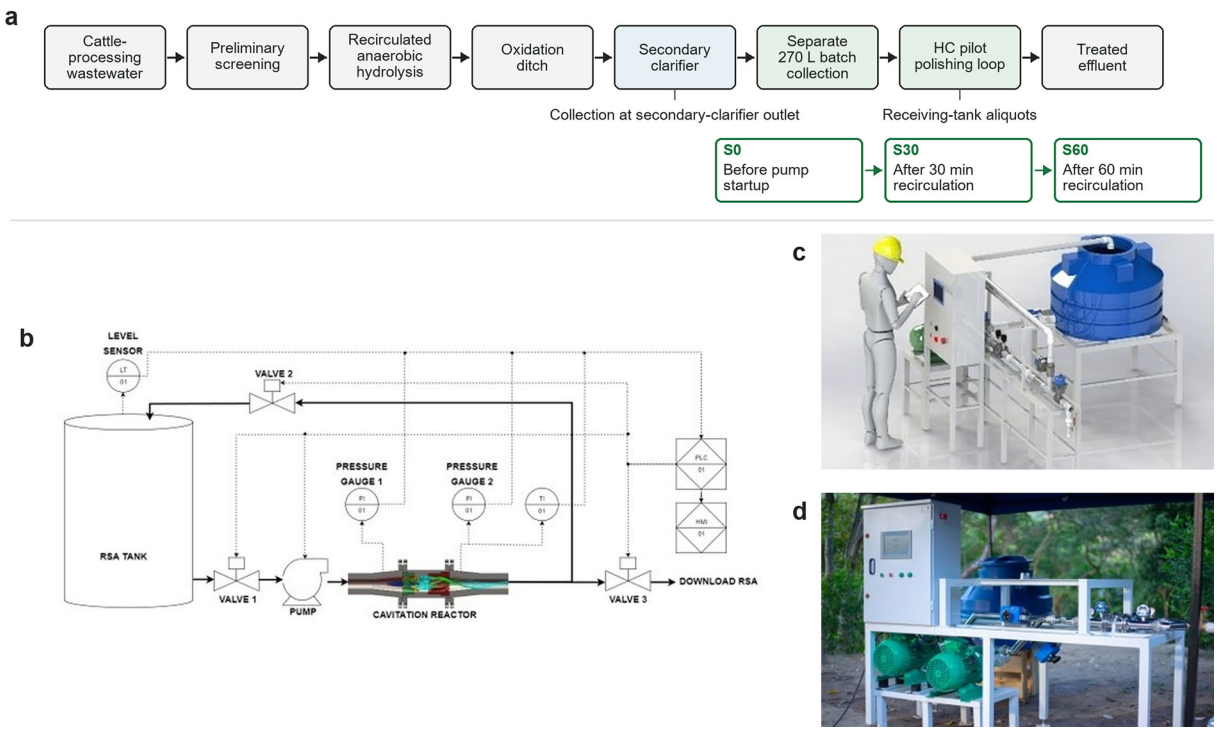

Figure 2. Location and configuration of the HC polishing step: (a) plant treatment train and aliquot sequence, showing collection from the secondary clarifier and sampling at 0, 30, and 60 min; (b) pilot process and instrumentation layout; (c) equipment model; and (d) assembled unit

omitted because local velocity and downstream absolute pressure were absent from the archived data. Without those terms and vapor pressure at the corresponding temperature, a retrospective value would not be reproducible.

Experimental design and sampling

Five field batches were treated as the independent experimental units. After the receiving tank was filled with a separate 270 L batch, the 0 min aliquot was collected before pump startup; the same batch was then recirculated for 60 min, with aliquots at 30 and 60 min. Temperature, upstream pressure, flow, and accumulated cycles were logged every 10 min. For each batch, time, and assay, three analytical determinations were averaged before comparison. Thus, $n = 5$ describes process replication; the three determinations describe measurement repeatability within a batch. Table 1 summarizes the batch design, sampling schedule, and recorded operating conditions.

We expressed recirculation as a nominal number of tank volumes, C:

$$C = Qt / V \quad (1)$$

In Equation 1, Q is mean flow in L s^{-1}, t is elapsed time in seconds, and V is the 270 L batch volume. The measured overall mean, $Q = 5.975$ L s^{-1}, gives one tank volume every 45.2 s. Sixty minutes therefore represents 21.5 m^3 of cumulative recirculation, equivalent to 79.7 tank volumes; the logged mean was 79.68 cycles. This ratio summarizes bulk pumping only. It contains no information on the residence-time distribution or on passage history for an individual fluid element.

Microbiological enumeration

Culture-based enumeration followed the applicable Standard Methods membrane-filtration procedures (American Public Health Association et al., 2017). The panel comprised the fecal- and total-coliform tests, aerobic mesophiles, and molds/yeasts. Depending on the anticipated abundance, a 10 mL portion was prepared at 10^{-3}, 10^{-6}, or 10^{-9} dilution and passed through a 47 mm, 0.45 µm nitrocellulose membrane. Each membrane was incubated on the medium assigned to that assay. Countable growth was converted to colony-forming units (CFU) 100 mL^{-1} from the filtered volume and dilution. Absence of growth on the selected plate was recorded as a non-detect under that procedure, without assigning sterility to the wastewater.

Table 1. Batch design and recorded operating conditions

Descriptor	Value or procedure
Wastewater matrix	Secondary-treated cattle slaughterhouse wastewater
Operating mode	Batch recirculation through a fin-type restriction
Working volume	270 L per independent run
Independent experimental units	Five treatment runs
Campaign period	Three months
Field-batch schedule	Five independent collections on different days and at different times of day; batches were not pooled
Treatment duration	60 min
Microbiological sampling	0, 30, and 60 min
Operational monitoring	Every 10 min
Analytical replication	Triplicate measurements within each run and time
Pump rating	Approximately 7.5 kW nominal nameplate power
Mean inlet pressure	680.3 ± 2.9 kPa
Mean flow	5.975 ± 0.178 L s^{-1}
Mean exposure at 60 min	79.68 ± 9.22 nominal tank-volume cycles

The source protocol records immediate processing of the water aliquots but does not log the exact collection-to-filtration interval in minutes or the collection-container material. These unrecorded details are reported as limitations rather than reconstructed retrospectively. The three determinations characterize repeatability for one batch–time combination and do not add independent HC runs. Both filtered volume and decimal dilution entered the conversion to a 100 mL basis. Variation among plates is analytical, whereas variation among the five field batches represents the observed process response to a non-uniform matrix.

Percentage reduction and treatment of non-detects

Percentage reduction (*PR*) was calculated from the pretreatment count (N_0) and the count after treatment (N) using Equation 2:

$$PR = 100 \times (N_0 - N) / N_0 \quad (2)$$

When the selected plate contained no colony, the percentage calculation rounded to 100%. That number remains constrained by the filtered volume and the dilution examined; it cannot demonstrate that the whole treated batch was sterile. We therefore report such endpoints as assay-specific non-detects and did not replace them with an imputed concentration for the final outcomes.

Near its 100% limit, PR loses resolution because several concentrations below the enumeration threshold produce the same rounded value. We therefore pair the percentage with the observed endpoint and its censoring qualification. Log reductions were omitted from the revised analysis: the aggregate laboratory file did not permit the earlier values to be reconciled with dilution records and zero-colony plates for each batch.

Statistical analysis

Results are summarized as mean ± standard deviation. The original analysis compared time points for temperature, upstream pressure, flow, and cumulative cycles by one-way analysis of variance (ANOVA) with Tukey-adjusted pairwise tests. Microbial counts, which included non-detects and substantial batch-to-batch dispersion, were evaluated with Kruskal–Wallis ranks followed by Dunn comparisons. The decision level was $\alpha = 0.05$. These tests preserve the available analytical record, but a one-factor analysis does not model repeated observations within the same batch. Accordingly, p-values are treated as exploratory and interpreted alongside the magnitude and dispersion of change and the censored culture observations.

RESULTS AND DISCUSSION

Initial wastewater characteristics

The water entering the pilot unit was not a dilute polishing matrix (Table 2). COD averaged 1561 mg O_2 L^{-1}, BOD_5 861.5 mg O_2 L^{-1},

and turbidity 425.2 nephelometric turbidity units (NTU); total solids were above 2 g L^{-1}. Both coliform groups began at approximately 10^7 CFU 100 mL^{-1}. Several reported standard deviations were large relative to their means, indicating substantial variability in the archived pretreatment measurements. Because the archived summary does not separate field-batch variability from analytical replication for every parameter, that dispersion is treated descriptively rather than assigned to a single variance component.

The mean BOD_5/COD ratio was approximately 0.55, indicating that a substantial biodegradable fraction remained after the reported biological treatment. At the same time, the mean total alkalinity was 2822.8 mg $CaCO_3$ L^{-1} and conductivity was 3802 µS cm^{-1}. These values describe a chemically buffered and ion-rich matrix in which chemical-radical pathways may not behave as they do in low-solids laboratory water. Because dissolved oxidants and radical probes were not measured, the baseline characterization is used to define matrix complexity rather than to assign a particular reaction pathway.

Microbial starting concentrations also differed by group: coliform and aerobic mesophile means were three orders of magnitude higher than the mean for molds and yeasts. Consequently, identical percentage reductions would not represent identical endpoint concentrations, and a single assay dilution would not provide the same resolution across all groups. The broad reported standard deviations—larger than the means for some parameters—also caution against selecting one inlet profile as representative. Treatment response is therefore summarized across the experimental runs rather than inferred from one nominal inlet concentration.

The inlet data in Table 2 describe the pretreatment samples recorded for the experimental campaign. They should not be interpreted as an annual average for the plant or as a typical composition for the sector. Published datasets differ in animal species, water use, treatment stage, and sampling scheme (Aziz et al., 2019; Michael et al., 2020). In this study, COD and turbidity define the matrix that actually entered the loop. That matrix is analytically relevant because dissolved and suspended matter can affect culture recovery and the environment in which cavitation occurs.

Hydraulic and thermal behavior

Two variables accumulated during operation (Figure 3). By 60 min, the batches had reached 79.68 ± 9.22 cycles and warmed by 19.5 ± 1.345 °C; the time effect for each was significant ($p < 0.001$). In contrast, upstream pressure and flow showed no significant time effect ($p > 0.05$), with overall means of 680.3 ± 2.9 kPa and 5.975 ± 0.178 L s^{-1}. Samples collected later in the run therefore came from warmer liquid with more accumulated passages, under a similar pressure-flow

Table 2. Characteristics measured before HC treatment; mean ± standard deviation as reported in the archived laboratory summary

Parameter	Mean ± SD
pH	8.064 ± 0.172
Temperature (°C)	27.4 ± 1.012
Turbidity (NTU)	425.2 ± 192.595
Conductivity (µS cm^{-1})	3802 ± 441
Total alkalinity (mg $CaCO_3$ L^{-1})	2822.8 ± 2260.643
BOD_5 (mg O_2 L^{-1})	861.5 ± 133.368
COD (mg O_2 L^{-1})	1561 ± 733.667
Total solids (mg L^{-1})	2224.8 ± 395.382
Settleable-solids volume (mL L^{-1})	0.26 ± 0.581
Suspended solids, total (mg L^{-1})	347.176 ± 140.231
Dissolved solids (mg L^{-1})	2099.068 ± 1076.975
Fecal-coliform count (CFU 100 mL^{-1})	$4.656 \times 10^7 \pm 5.330 \times 10^7$
Total-coliform count (CFU 100 mL^{-1})	$5.638 \times 10^7 \pm 5.134 \times 10^7$
Aerobic mesophilic bacteria (CFU 100 mL^{-1})	$3.226 \times 10^7 \pm 2.427 \times 10^7$
Molds and yeasts (CFU 100 mL^{-1})	$7.364 \times 10^4 \pm 6.129 \times 10^4$

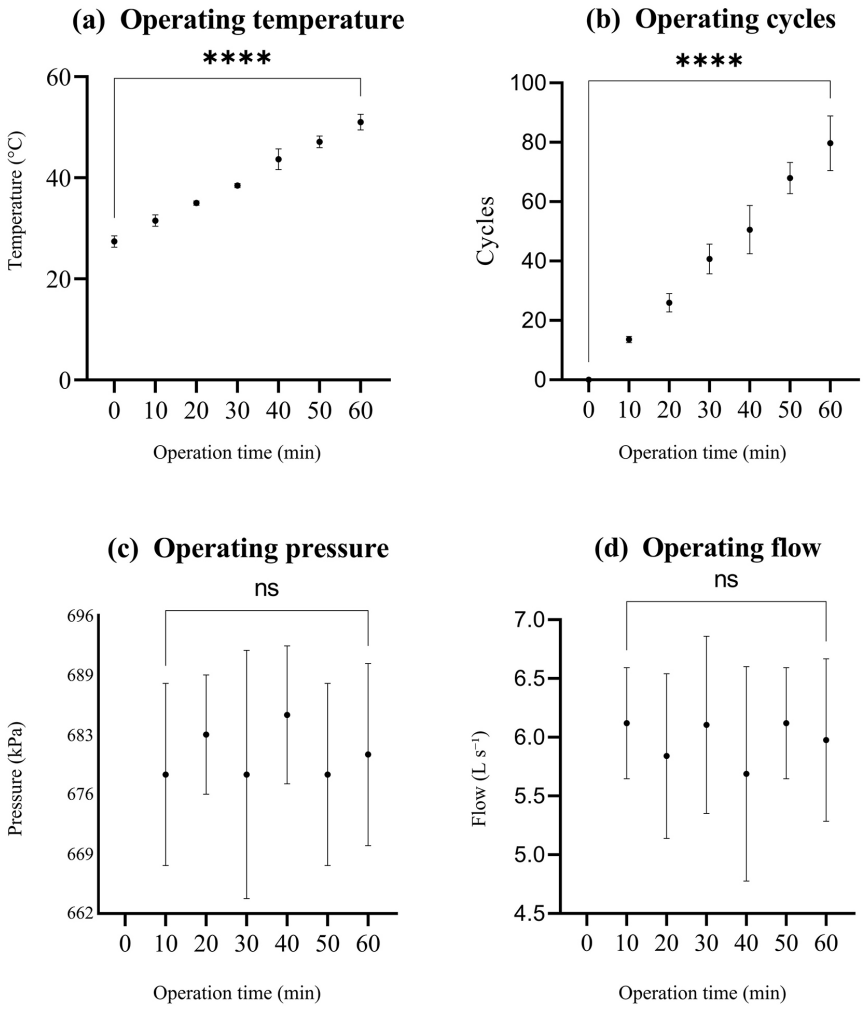

Figure 3. Time course of (a) bulk temperature, (b) accumulated tank-volume cycles, (c) upstream pressure, and (d) flow during the 60 min batches. All plotted quantities are expressed in SI units; upstream pressure was converted from the original gauge scale to kPa for presentation. Symbols are five-batch means and bars summarize between-batch variation. Significance labels reproduce the exploratory one-factor ANOVA and Tukey output (****, reported $p < 0.001$; ns, $p > 0.05$)

setting. Passage number and heating remain inseparable in these data. Mean flow corresponds to approximately 1.33 tank volumes min^{-1}. Its 60 min integral agrees closely with the recorded cycle total, supporting consistency of the bulk flow record. Agreement at that level cannot reveal bypassing, dead zones, or the distribution of passes through the fin. Those features require tracer measurements and residence-time analysis before the loop geometry is scaled. Published pressure ranges provide context rather than an optimum for this reactor. Municipal-wastewater response varied among 3.5, 5, and 7 bar in Lebiocka (2020). For sludge disintegration, Ahmed et al. (2025) found that pressure interacted with the orifice arrangement. Both findings are apparatus- and matrix-dependent. Because pressure and flow remained stable in our trials, the microbial difference between 30 and 60 min coincided with additional circulation and higher temperature, not with an altered hydraulic set point. Mean bulk temperature increased from 27.4 °C to approximately 46.9 °C. Although 46.9 °C is below a conventional pasteurization condition, this rise can change membrane state and culture recovery as well as liquid viscosity, vapor pressure, and cavitation behavior. The study had no non-cavitating loop with a matched thermal profile. Accordingly, the observed microbial response applies to the combined recirculating system; the portions attributable to the fin, the pump, and heating are unknown.

The upstream gauge reading does not reconstruct cavitation intensity. Cavitation number depends on the pressure and velocity definitions

used, while geometry, temperature, dissolved gas, and nuclei also shape the regime (Šarc et al., 2017). Burzio et al. (2020) found an inverse association with *E. coli* inactivation within their orifice apparatus. That apparatus-specific relationship cannot be treated as a threshold for the fin. We excluded a retrospective estimate because the archived record lacks local velocity and downstream absolute pressure.

Microbial response

Counts declined in each culture group, but the batches entered treatment with broad dispersion (Figure 4). After adjustment for multiple comparisons, pretreatment differed from 60 min ($p < 0.05$). The two adjacent contrasts, 0–30 and 30–60 min, were not significant for every group. With only five batches and one intermediate

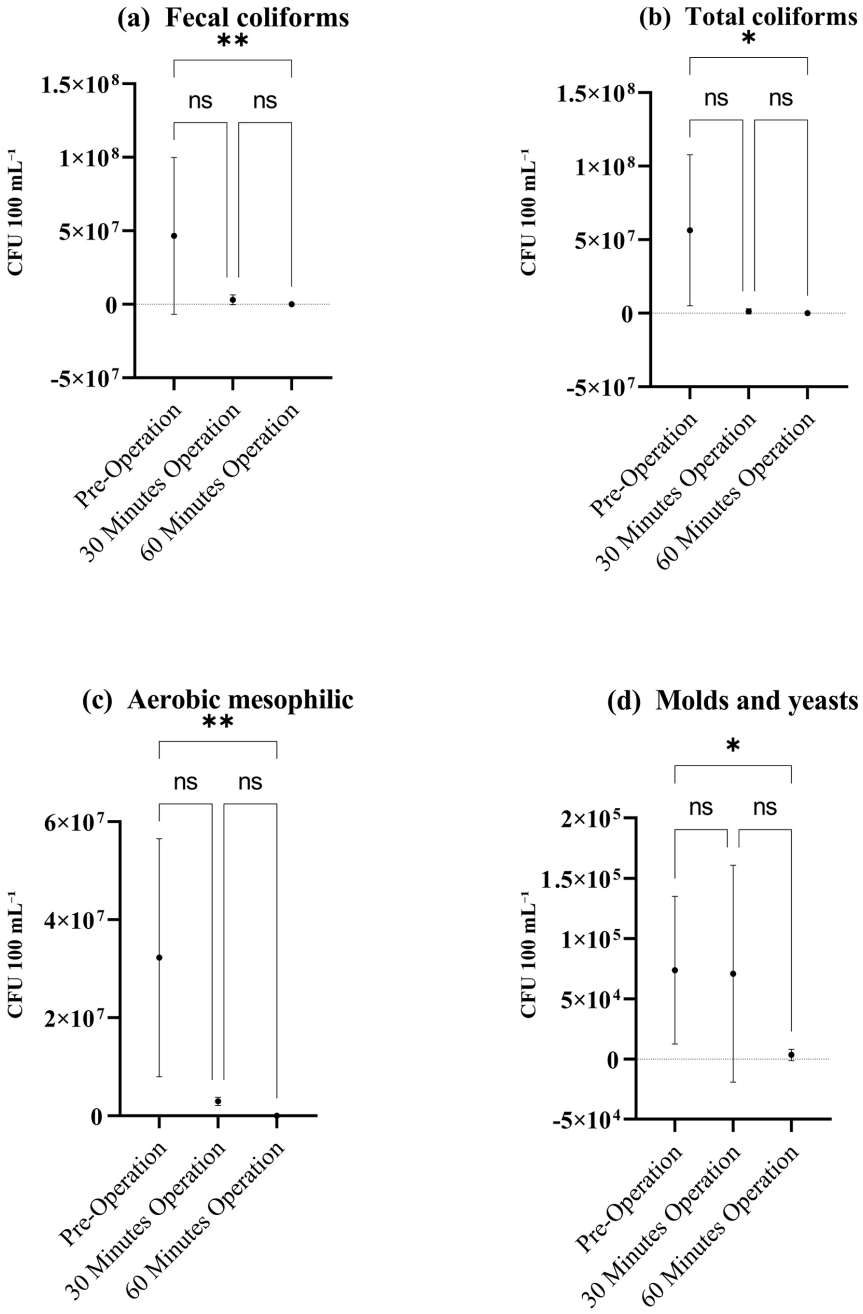

Figure 4. Culture results across the five batches at 0, 30, and 60 min: (a) fecal-coliform assay, (b) total-coliform assay, (c) aerobic-mesophile assay, and (d) mold/yeast assay. Markers denote means and vertical bars summarize variation among batches. Brackets reproduce exploratory Dunn comparisons following Kruskal–Wallis testing (ns, non-significant; one asterisk, $p < 0.05$; two asterisks, $p < 0.01$). Where a symmetric error bar crosses zero, its negative segment reflects the dispersion summary and does not denote a negative colony count

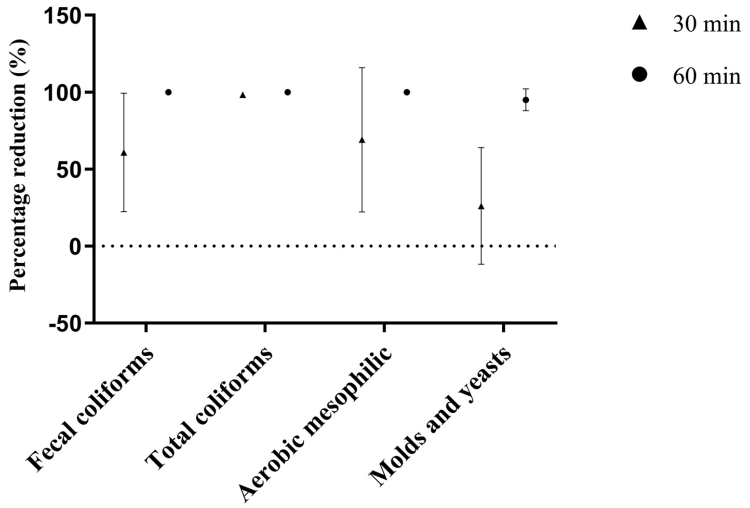

Figure 5. Percentage reduction from the initial count at 30 and 60 min. Points show means across batches and bars show between-run variation. A 100% plotted endpoint is the rounded result of a plate without colonies under the selected assay, not proof of complete absence

microbiological sample, we interpret the full-period change more confidently than the apparent shape of the response between sampling points.

At 30 min, mean percentage reductions were 60.855 ± 38.463% for fecal coliforms, 98.311 ± 1.755% for total coliforms, 69.106 ± 46.913% for aerobic mesophilic bacteria, and 26.09 ± 37.871% for molds and yeasts. At 60 min, no colonies were detected under the assay conditions for the first three groups, and molds and yeasts decreased by 95.0 ± 7.071% (Figure 5). The non-detects and rounded 100% values should not be described as complete elimination because neither recovery tests nor post-treatment regrowth assays were performed. The 30 min sample did not rank the indicators uniformly. Total coliforms had the largest mean reduction and the narrowest dispersion; molds and yeasts changed least at that point and were still culturable after 60 min. Fecal coliforms and aerobic mesophiles varied widely among batches at 30 min. A common elapsed time therefore did not produce a common early response. For that reason, we retain group-specific results instead of collapsing bacteria and fungi into one microbial-load value.

Persistence of molds and yeasts could reflect group-level resistance, but the experiment did not test cellular structure. Initial abundance, aggregation, attachment to solids, recovery in culture, and dilution resolution are alternative explanations for an apparently slower response. The defensible observation is therefore limited to different trajectories among the four assays; the dataset does not assign them to a particular cell-injury pathway.

Published experiments point in the same direction without resolving the mechanism here. Vortex-diode and supercavitation studies found unequal responses across bacteria with different envelope structures (Jain et al., 2019; Šarc et al., 2018). Kosel et al. (2017) demonstrated viral inactivation, but for another target and enumeration method. At the opposite spatial scale, Pandur et al. (2023) showed that lethal microjet effects occur in a narrow bubble-cell interaction zone. Our four-indicator panel extends the observation beyond one bacterial strain, but it neither measures exposure of individual cells nor establishes pathogen-specific susceptibility. For three groups, the 60 min plates yielded non-detects. This is operationally relevant only within the assay threshold; it does not establish compliance unless that threshold is lower than the applicable discharge or reuse limit. Specific pathogens, viable-but-nonculturable cells, and regrowth were outside the experiment. The microbiological finding is therefore an immediate post-treatment reduction in culturable indicators under the reported procedure.

A related pilot study with urban wastewater reported decreases in the same culture assays (Cobos Ramírez et al., 2026). The values are not directly comparable because geometry, flow history, batch volume, and starting counts differed. Slaughterhouse solids and dissolved organic matter may protect cells or consume reactive species, whereas recirculation increases the chance that a cell traverses the active region (Hou et al., 2023; Sun et al., 2020). A quantitative comparison

would require identical detection limits and energy measured on a common basis.

The urban and slaughterhouse studies share investigators and analytical endpoints, and they began with different solids, organic loads, and counts. They were not concurrent arms of one experiment. Consequently, any difference may reflect protocol or equipment as well as matrix. The limited cross-study result is that related field units produced measurable changes in culturable indicators for two real wastewaters. No mechanistic endpoint was measured in these trials. The literature describes membrane injury from shear or microjets and reactions within transient chemical microenvironments (Zupanc et al., 2019). Sikora et al. (2026) measured hydroxyl-radical formation independently. We used neither a radical probe nor a cellular-damage assay, and time was correlated with circulation and temperature. The data show lower culturable abundance after longer loop operation, without identifying which pathway contributed most.

The installed pump had an approximate nominal nameplate rating of 7.5 kW, but power draw was not recorded. The nameplate therefore cannot be converted into batch energy without load and efficiency measurements. The calculated 21.5 m^3 is likewise a hydraulic quantity: it is the volume moved cumulatively around a closed 270 L batch, rather than product throughput or energy dose. The retained measurements permit hydraulic and microbiological analysis, not an energy assessment.

HC studies report energy as electricity per volume, energy per log reduction, cost per cubic metre, or sometimes nameplate power alone. The absence of one denominator obstructs scale comparison (Agarkoti et al., 2021; Sun et al., 2024). Published cavitation reactors treating synthetic or domestic water do not supply the missing value for this 270 L fin reactor (Yadav et al., 2021). Future runs should record voltage, current, power factor or shaft power, throughput, and auxiliary demand over the same interval used for culture sampling.

Cross-study context and study limitations

Table 3 places the present result beside selected polishing treatments reported for slaughterhouse wastewater. The comparison is descriptive because the studies used different matrices, volumes, analytical methods, and reporting thresholds. The principal contribution of the present work is the treatment of a 270 L real effluent batch, rather than evidence that HC is intrinsically superior to electrocoagulation, UV-C, ozone, or acoustic cavitation.

The table also shows why an endpoint reported as zero cannot be compared without the corresponding analyzed volume and detection threshold. For example, hybrid electrocoagulation–membrane–UV treatment and membrane-based polishing can achieve strong removal in poultry wastewater, but their process trains, dose metrics, and separation mechanisms differ from HC (Fatima et al., 2021; Meiramkulova et al., 2021). Similarly, ozonation-assisted acoustic cavitation includes an oxidant dose and cannot be treated as acoustic energy alone (Alfonso-Muniozguren et al., 2020). The appropriate inference is therefore comparative context, not technological superiority. Table 4 summarizes the evidence used to delimit the inferences permitted by this dataset.

Several features delimit the claim. The archived laboratory file does not contain endpoint-specific enumeration thresholds or the complete media and incubation conditions; it records immediate processing but not the exact collection-to-filtration interval in minutes. Consequently, non-detects remain censored and the culture procedure is not fully reproducible from that file alone. The process dataset comprises five batches sampled

Table 3. Descriptive cross-study comparison of reported microbial outcomes for selected slaughterhouse-wastewater polishing treatments. Values are reproduced for context and are not energy- or detection-limit-normalized

Treatment	Volume (L)	Time (min)	Initial total coliforms (CFU 100 mL^{-1})	Reported endpoint	Source
Hydrodynamic cavitation	270	60	5.638×10^7	Total coliforms not detected under assay conditions	Present study
Electrocoagulation	3	150	1.23×10^7	68.76 CFU 100 mL^{-1}	Sandoval et al. (2024)
UV-C	0.2	60	7.3×10^4	Non-detect reported	Svierzoski et al. (2021)
Ozonation	0.4	60	4.45×10^3	Non-detect reported	Alfonso-Muniozguren et al. (2020)
Acoustic cavitation	0.4	60	4.45×10^3	4.05×10^3 CFU 100 mL^{-1}	Alfonso-Muniozguren et al. (2020)

Table 4. Evidence-based interpretation framework for the present pilot study

Factor	Evidence from the literature	Present-study descriptor	Permitted inference
Wastewater matrix	Slaughterhouse composition varies with process and treatment stage (Aziz et al., 2019; Yaakob et al., 2018)	Real secondary effluent; COD 1561 mg O_2 L^{-1}; turbidity 425.2 NTU	Feasibility applies to the characterized runs, not all slaughterhouses
Reactor geometry	Restriction and rotor–stator geometry change cavitation and inactivation (Jain et al., 2019; Xue et al., 2025)	Recirculating fin-type restriction	Performance is device-specific
Hydraulic exposure	Flow and passage frequency affect contact with active zones (Hou et al., 2023)	79.68 ± 9.22 nominal tank-volume cycles at 60 min	Cycles supplement time but are not a residence-time distribution
Cavitation regime	Cavitation number alone is insufficient without full definitions and geometry (Šarc et al., 2017)	Inlet pressure measured; local velocity and downstream absolute pressure unavailable	No defensible cavitation-number claim
Thermal co-exposure	Bulk heating can contribute to rotational-HC disinfection (Sun et al., 2018)	Mean temperature increase 19.5 ± 1.345 °C	Integrated HC response; thermal contribution not isolated
Microbial endpoint	Organisms and cavitation regimes produce different responses (Jain et al., 2019; Zupanc et al., 2019)	Four culture-based indicator groups; three non-detects at 60 min	Indicator reduction, not sterilization or pathogen absence
Energy and scale	Energy-normalized validation is required for industrialization (Agarkoti et al., 2021; Sun et al., 2024)	Approximately 7.5 kW nameplate only; actual power not measured	No energy-efficiency, cost, or sustainability claim

for culture at three times. Its original one-factor tests also omit correlation within batches, so the associated p-values are exploratory. No temperature-matched or non-cavitating circulation control was run, regrowth was not monitored, and electricity, cavitation number, dissolved oxygen, and reactive species were not measured. The supported claim is limited to microbial reduction in the tested pilot batches. Sterility, process optimization, energy advantage, mechanistic exclusivity, and sustainability require additional evidence.

Five 270 L field runs provide a different level of evidence from a single-species bench suspension. Culture results, hydraulic variables, and temperature were measured for each real-effluent batch. Tank-volume circulation records repeated passage quantitatively. Equally important, the analysis counts batches as process replicates and plates as repeated analytical measurements. On that basis, the study supports feasibility and specifies what a confirmatory experiment must add: appropriate controls and direct power measurement.

CONCLUSIONS

All four culture assays declined across the five independently treated 270 L batches of secondary slaughterhouse effluent. The 60 min point provided the highest observed microbiological performance: no colony was recovered in either coliform assay or in the aerobic-mesophile assay under the specified culture procedures, whereas molds/yeasts decreased by 95.0 ± 7.071%. These zero-colony observations are reported as assay-specific non-detects rather than evidence of sterility. At 30 min, mean reductions ranged from 26.09% for molds/yeasts to 98.311% for total coliforms. During treatment, upstream pressure averaged 680.3 ± 2.9 kPa and flow averaged 5.975 ± 0.178 L s^{-1} without a significant time effect, while bulk temperature increased by 19.5 ± 1.345 °C and cumulative exposure reached 79.68 ± 9.22 tank-volume cycles. The hydraulic stability of the loop accompanied a progressively greater microbial response with recirculation time under the combined hydraulic and thermal conditions of the pilot system.

The principal novelty is the repeated evaluation of five real-effluent batches collected over three months on different days and at different times of day, treated at a 270 L pilot volume through the same fin-type restriction, and assessed with four culture endpoints and a concurrent hydraulic–thermal record. By integrating temporal batch replication with hydraulic, thermal, and microbiological measurements, the design moves beyond a descriptive reactor trial and shows that the direction of the microbial response persisted across independently collected field batches. The practical impact is a field-based operating benchmark: among the conditions tested, 60 min produced the strongest microbiological outcome while pressure and flow remained stable. The findings support the fin-reactor loop as a candidate tertiary-polishing step for secondary

slaughterhouse effluent within the tested operating envelope. Together, the results provide pilot-scale evidence of feasibility and repeatability and a defined operating reference for comparable secondary-effluent conditions.

Acknowledgements

The project was executed by UNISANGIL. The authors thank the Gobernación de Santander, Alcaldía de San Gil, Cámara de Comercio de Bucaramanga, Corporación Autónoma Regional de Santander, Universidad de Santander, Universidad Santo Tomás, and Universidad Autónoma de Bucaramanga for their collaboration.

REFERENCES

1. Agarkoti, C., Thanekar, P. D., Gogate, P. R. (2021). Cavitation-based treatment of industrial wastewater: A critical review focusing on mechanisms, design aspects, operating conditions and application to real effluents. *Journal of Environmental Management, 300*, 113786. https://doi.org/10.1016/j.jenvman.2021.113786
2. Ahmed, D., Aboulfotoh, A. M., Elsafty, Z. (2025). Harnessing hydrodynamic cavitation, alkaline treatments and advanced oxidation processes for enhancement of sludge disintegration. *Journal of Ecological Engineering, 26*(10), 374–388. https://doi.org/10.12911/22998993/207192
3. Alfonso-Muniozguren, P., Hazzwan Bohari, M., Sicilia, A., Avignone-Rossa, C., Bussemaker, M., Saroj, D., Lee, J. (2020). Tertiary treatment of real abattoir wastewater using combined acoustic cavitation and ozonation. *Ultrasonics Sonochemistry, 64*, 104986. https://doi.org/10.1016/j.ultsonch.2020.104986
4. American Public Health Association, American Water Works Association, & Water Environment Federation. (2017). *Standard methods for the examination of water and wastewater* (23rd ed.). American Public Health Association.
5. Asgharnejad, H., Khorshidi Nazloo, E., Madani Larijani, M., Hajinajaf, N., Rashidi, H. (2021). Comprehensive review of water management and wastewater treatment in food processing industries in the framework of water–food–environment nexus. *Comprehensive Reviews in Food Science and Food Safety, 20*(5), 4779–4815. https://doi.org/10.1111/1541-4337.12782
6. Aziz, A., Basheer, F., Sengar, A., Irfanullah, Khan, S. U., Farooqi, I. H. (2019). Biological wastewater treatment (anaerobic–aerobic) technologies for safe discharge of treated slaughterhouse and meat processing wastewater. *Science of the Total Environment, 686*, 681–708. https://doi.org/10.1016/j.scitotenv.2019.05.295
7. Burzio, E., Bersani, F., Caridi, G. C. A., Vesipa, R., Ridolfi, L., Manes, C. (2020). Water disinfection by orifice-induced hydrodynamic cavitation. *Ultrasonics Sonochemistry, 60*, 104740. https://doi.org/10.1016/j.ultsonch.2019.104740
8. Bustillo-Lecompte, C., Mehrvar, M. (2017). Slaughterhouse wastewater: Treatment, management and resource recovery. In M. N. V. Prasad & K. Shih (Eds.), *Physico-chemical wastewater treatment and resource recovery* (pp. 153–174). IntechOpen. https://doi.org/10.5772/65499
9. Carpenter, J., Badve, M., Rajoriya, S., George, S., Saharan, V. K., Pandit, A. B. (2017). Hydrodynamic cavitation: An emerging technology for the intensification of various chemical and physical processes in a chemical process industry. *Reviews in Chemical Engineering, 33*(5), 433–468. https://doi.org/10.1515/revce-2016-0032
10. Cerecedo, L. M., Dopazo, C., Gomez-Lus, R. (2018). Water disinfection by hydrodynamic cavitation in a rotor–stator device. *Ultrasonics Sonochemistry, 48*, 71–78. https://doi.org/10.1016/j.ultsonch.2018.05.015
11. Chen, Y., Yin, C., Song, Y. (2023). Application of hydrodynamic cavitation in the field of water treatment. *Chemical Papers, 77*, 3521–3546. https://doi.org/10.1007/s11696-023-02754-y
12. Cobos Ramírez, L. E., Muñoz Neira, M. J., Benítez Muñoz, S. J., Neira Tavera, J. A., Vargas Tangua, F. C., Mendoza Castellanos, L. S., Jara Mora, F. A., Ayala Ramírez, A., Dueñas Bohórquez, F. A., Gamboa Contreras, W. (2026). Novel hydrodynamic cavitation system for microorganism reduction in urban wastewater discharged over Fonce River. *Journal of Ecological Engineering, 27*(4), 310–323. https://doi.org/10.12911/22998993/213506
13. Collivignarelli, M. C., Abbà, A., Benigna, I., Sorlini, S., Torretta, V. (2018). Overview of the main disinfection processes for wastewater and drinking water treatment plants. *Sustainability, 10*(1), 86. https://doi.org/10.3390/su10010086
14. Costa, M., Terrón, D., Leal, C., Pazos, M., Sanromán, A., Ferreira, E. C., Quintelas, C. (2026). Disinfection in wastewater treatment: From conventional to emerging technologies. *Journal of Water Process Engineering, 87*, 110070. https://doi.org/10.1016/j.jwpe.2026.110070
15. Dos Santos Pereira, A. K., Teixeira, K. C., Pereira, D. H., Cavallini, G. S. (2024). A critical review on slaughterhouse wastewater: Treatment methods and reuse possibilities. *Journal of Water Process Engineering, 58*, 104819. https://doi.org/10.1016/j.jwpe.2024.104819
16. Dular, M., Griessler-Bulc, T., Gutierrez-Aguirre, I.,

Heath, E., Kosjek, T., Krivograd Klemenčič, A., Oder, M., Petkovšek, M., Rački, N., Ravnikar, M., Šarc, A., Širok, B., Zupanc, M., Žitnik, M., Kompare, B. (2016). Use of hydrodynamic cavitation in (waste)water treatment. *Ultrasonics Sonochemistry, 29*, 577–588. https://doi.org/10.1016/j.ultsonch.2015.10.010

17. Elsaidy, N. R., Elleboudy, N. S., Alkhedaide, A., Abouelenien, F. A., Abdelrahman, M. H., Soliman, M. M., & Shukry, M. (2022). Enhancement effects of water magnetization and/or disinfection by sodium hypochlorite on secondary slaughterhouse wastewater effluent quality and disinfection by-products. *Processes, 10*(8), 1589. https://doi.org/10.3390/pr10081589
18. Fatima, F., Du, H., Kommalapati, R. R. (2021). Treatment of poultry slaughterhouse wastewater with membrane technologies: A review. *Water, 13*(14), 1905. https://doi.org/10.3390/w13141905
19. Gode, A., Madane, K., Ranade, V. V. (2023). Design of vortex-based cavitation devices/reactors: Influence of aspect ratio, number of inlets and shape. *Ultrasonics Sonochemistry, 101*, 106695. https://doi.org/10.1016/j.ultsonch.2023.106695
20. González, Y., Gómez, G., Moeller-Chávez, G. E., Vidal, G. (2023). UV disinfection systems for wastewater treatment: Emphasis on reactivation of microorganisms. *Sustainability, 15*(14), 11262. https://doi.org/10.3390/su151411262
21. Gostiša, J., Drešar, P., Hočevar, M., Dular, M. (2022). Computational analysis of flow conditions in hydrodynamic cavitation generator for water treatment processes. *Canadian Journal of Chemical Engineering, 100*(12), 3502–3516. https://doi.org/10.1002/cjce.24572
22. Goswami, K. P., Pugazhenthi, G. (2020). Treatment of poultry slaughterhouse wastewater using tubular microfiltration membrane with fly ash as key precursor. *Journal of Water Process Engineering, 37*, 101361. https://doi.org/10.1016/j.jwpe.2020.101361
23. Hong, F., Tian, H., Yuan, X., Liu, S., Peng, Q., Shi, Y., Jin, L., Ye, L., Jia, J., Ying, D., Thomas, S. R., Huang, Y. (2022). CFD-assisted modeling of hydrodynamic cavitation reactors for wastewater treatment—A review. *Journal of Environmental Management, 321*, 115982. https://doi.org/10.1016/j.jenvman.2022.115982
24. Hou, R., Song, Y., Liu, J., Zhang, L., Zhang, M., Sun, X. (2023). Experimental and numerical investigation on the disinfection characteristics of a novel rotor-radial groove hydrodynamic cavitation reactor. *Process Safety and Environmental Protection, 169*, 260–269. https://doi.org/10.1016/j.psep.2022.11.019
25. Igbinosa, I. H., Uwidia, I. E. (2018). Effect of abattoir effluents on the physicochemical properties of a receiving watershed in an urban community. *Ife Journal of Science, 20*(2), 219–228. https://doi.org/10.4314/ijs.v20i2.2
26. Jain, P., Bhandari, V. M., Balapure, K., Jena, J., Ranade, V. V., Killedar, D. J. (2019). Hydrodynamic cavitation using vortex diode: An efficient approach for elimination of pathogenic bacteria from water. *Journal of Environmental Management, 242*, 210–219. https://doi.org/10.1016/j.jenvman.2019.04.057
27. Kosel, J., Gutierrez-Aguirre, I., Rački, N., Dreo, T., Ravnikar, M., Dular, M. (2017). Efficient inactivation of MS-2 virus in water by hydrodynamic cavitation. *Water Research, 124*, 465–471. https://doi.org/10.1016/j.watres.2017.07.077
28. Lebiocka, M. (2020). Application of hydrodynamic cavitation to improve the biodegradability of municipal wastewater. *Journal of Ecological Engineering, 21*(6), 155–160. https://doi.org/10.12911/22998993/123163
29. Lopes, C. L., de Assis, T. M., Passig, F. H., Lima Model, A. N., Mees, J. B. R., Cervantes, F. J., Gotardo, J. T., Gomes, S. D. (2022). Nitrogen removal from poultry slaughterhouse wastewater in anaerobic-anoxic-aerobic combined reactor: Integrated effect of recirculation rate and hydraulic retention time. *Journal of Environmental Management, 303*, 114–162. https://doi.org/10.1016/j.jenvman.2021.114162
30. Mane, M. B., Bhandari, V. M., Balapure, K., Ranade, V. V. (2020). Destroying antimicrobial resistant bacteria and difficult, opportunistic pathogen using cavitation and natural oils/plant extract. *Ultrasonics Sonochemistry, 69*, 105272. https://doi.org/10.1016/j.ultsonch.2020.105272
31. Meiramkulova, K., Temirbekova, A., Saspugayeva, G., Kydyrbekova, A., Devrishov, D., Tulegenova, Z., Aubakirova, K., Kovalchuk, N., Meirbekov, A., Mkilima, T. (2021). Performance of a combined treatment approach on the elimination of microbes from poultry slaughterhouse wastewater. *Sustainability, 13*(6), 3467. https://doi.org/10.3390/su13063467
32. Michael, S., Paschal, C., Kivevele, T., Rwiza, M. J., Njau, K. N. (2020). Performance investigation of the slaughterhouse wastewater treatment facility: A case of Mwanza City Slaughterhouse, Tanzania. *Water Practice & Technology, 15*(4), 1096–1110. https://doi.org/10.2166/wpt.2020.085
33. Muñoz Neira, M. J., Gamboa Contreras, W., Vargas Tangua, F. C., Jara Mora, F. A., Neira Tavera, J. A., Cobos Ramírez, L. E., Ramírez Ordoñez, Y., Dueñas Bohórquez, F. A., Ayala Ramírez, A., Benítez Muñoz, S. J., Martínez Santana, Y. M., Peña Perea, S. A., Holkar, C. R., Jadhav, A. J., Pandit, A. B. (2025). *Cavitación hidrodinámica para el tratamiento de vertidos no convencionales [Hydrodynamic cavitation for the treatment of non-conventional effluents]* (in Spanish). UNISANGIL Editora.
34. Pandur, Ž., Zevnik, J., Podbevšek, D., Stojković, B., Stopar, D., Dular, M. (2023). Water treatment by cavitation: Understanding it at a single bubble–bacterial cell level. *Water Research, 236*, 119956.

https://doi.org/10.1016/j.watres.2023.119956

35. Patil, Y., Sonawane, S. H., Shyam, P., Sun, X., Manickam, S. (2023). Hybrid hydrodynamic cavitation technique for the treatment and disinfection of lake water. *Ultrasonics Sonochemistry, 97*, 106454. https://doi.org/10.1016/j.ultsonch.2023.106454
36. Salve, A. R., Pegu, K., Arya, S. S. (2019). Comparative assessment of high-intensity ultrasound and hydrodynamic cavitation processing on physico-chemical properties and microbial inactivation of peanut milk. *Ultrasonics Sonochemistry, 59*, 104728. https://doi.org/10.1016/j.ultsonch.2019.104728
37. Sandoval, M. A., Coreño, O., García, V., Salazar-González, R. (2024). Enhancing industrial swine slaughterhouse wastewater treatment: Optimization of electrocoagulation technique and operating mode. *Journal of Environmental Management, 349*, 119556. https://doi.org/10.1016/j.jenvman.2023.119556
38. Šarc, A., Stepišnik-Perdih, T., Petkovšek, M., Dular, M. (2017). The issue of cavitation number value in studies of water treatment by hydrodynamic cavitation. *Ultrasonics Sonochemistry, 34*, 51–59. https://doi.org/10.1016/j.ultsonch.2016.05.020
39. Šarc, A., Kosel, J., Stopar, D., Oder, M., Dular, M. (2018). Removal of bacteria *Legionella pneumophila*, *Escherichia coli*, and *Bacillus subtilis* by (super) cavitation. *Ultrasonics Sonochemistry, 42*, 228–236. https://doi.org/10.1016/j.ultsonch.2017.11.004
40. Sikora, P., Fialová, S., Pochylý, F., Maršálková, E. (2026). Theoretical framework and preliminary experimental evaluation of magnetically enhanced production of hydroxyl radicals in cavitating flows for wastewater treatment. *Journal of Ecological Engineering, 27*(3), 274–287. https://doi.org/10.12911/22998993/213631
41. Stošić, M., Čučak, D., Kovačević, S., Perović, M., Radonić, J., Turk Sekulić, M., Vojinović Miloradov, M., Radnović, D. (2016). Meat industry wastewater: Microbiological quality and antimicrobial susceptibility of *E. coli* and *Salmonella* sp. isolates, case study in Vojvodina, Serbia. *Water Science and Technology, 73*(10), 2509–2517. https://doi.org/10.2166/wst.2016.113
42. Sun, X., Park, J. J., Kim, H. S., Lee, S. H., Seong, S. J., Om, A. S., Yoon, J. Y. (2018). Experimental investigation of the thermal and disinfection performances of a novel hydrodynamic cavitation reactor. *Ultrasonics Sonochemistry, 49*, 13–23. https://doi.org/10.1016/j.ultsonch.2018.02.039
43. Sun, X., Liu, J., Ji, L., Wang, G., Zhao, S., Yoon, J. Y., Chen, S. (2020). A review on hydrodynamic cavitation disinfection: The current state of knowledge. *Science of the Total Environment, 737*, 139606. https://doi.org/10.1016/j.scitotenv.2020.139606
44. Sun, X., Xu, H., Xuan, X., Manickam, S., Boczkaj, G., Wang, B. (2024). Assessing the industrialization progress of hydrodynamic cavitation process intensification technology: A review. *Current Opinion in Chemical Engineering, 45*, 101037. https://doi.org/10.1016/j.coche.2024.101037
45. Svierzoski, N. D. S., Matheus, M. C., Bassin, J. P., Brito, Y. D., Mahler, C. F., Webler, A. D. (2021). Treatment of slaughterhouse wastewater by anoxic–aerobic biological reactors followed by UV-C disinfection and microalgae bioremediation. *Water Environment Research, 93*(3), 409–420. https://doi.org/10.1002/wer.1435
46. von Gunten, U. (2018). Oxidation processes in water treatment: Are we on track? *Environmental Science & Technology, 52*(9), 5062–5075. https://doi.org/10.1021/acs.est.8b00586
47. Xue, L., Hao, Z., Manickam, S., Liu, G., Wang, H., Sun, X., Bie, H. (2025). Evaluation of disinfection and cavitation performance of a cylindrical rotational hydrodynamic cavitation reactor: Influence of key geometric parameters of the cavitation generation unit. *Ultrasonics Sonochemistry, 121*, 107544. https://doi.org/10.1016/j.ultsonch.2025.107544
48. Yaakob, M. A., Radin Mohamed, R. M. S., Al-Gheethi, A. A. S., Mohd Kassim, A. H. (2018). Characteristics of chicken slaughterhouse wastewater. *Chemical Engineering Transactions, 63*, 637–642. https://doi.org/10.3303/CET1863107
49. Yadav, M., Sharma, J., Yadav, R. K., Gole, V. L. (2021). Microbial disinfection of water using hydrodynamic cavitational reactors. *Journal of Water Process Engineering, 41*, 102097. https://doi.org/10.1016/j.jwpe.2021.102097
50. Zarei, A., Biglari, H., Mobini, M., Dargahi, A., Ebrahimzadeh, G., Naroie, M. R., Mehrizi, E. A., Yari, A. R., Mohammadi, M. J., Baneshi, M. M., Khosravi, R., Poursadeghiyan, M. (2018). Disinfecting poultry slaughterhouse wastewater using copper electrodes in the electrocoagulation process. *Polish Journal of Environmental Studies, 27*(4), 1907–1912. https://doi.org/10.15244/pjoes/78150
51. Zheng, H., Zheng, Y., Zhu, J. (2022). Recent developments in hydrodynamic cavitation reactors: Cavitation mechanism, reactor design, and applications. *Engineering, 19*, 180–198. https://doi.org/10.1016/j.eng.2022.04.027
52. Zupanc, M., Pandur, Ž., Stepišnik Perdih, T., Stopar, D., Petkovšek, M., Dular, M. (2019). Effects of cavitation on different microorganisms: The current understanding of the mechanisms taking place behind the phenomenon. A review and proposals for further research. *Ultrasonics Sonochemistry, 57*, 147–165. https://doi.org/10.1016/j.ultsonch.2019.05.009